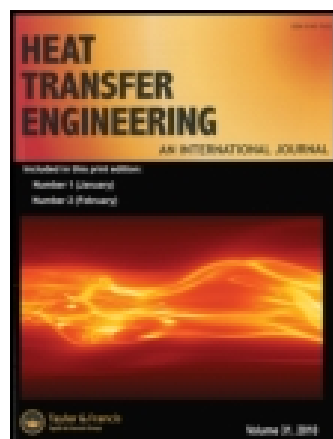


On: 30 March 2015, At: 06:11

Publisher: Taylor & Francis

Informa Ltd Registered in England and Wales Registered Number: 1072954 Registered office: Mortimer House, 37-41 Mortimer Street, London W1T 3JH, UK



## Heat Transfer Engineering

Publication details, including instructions for authors and subscription information:

<http://www.tandfonline.com/loi/uhte20>

### Pool Boiling on Modified Surfaces Using R-123

Syed W. Ahmad<sup>a</sup>, John S. Lewis<sup>b</sup>, Ryan J. McGlen<sup>c</sup> & Tassos G. Karayiannis<sup>b</sup>

<sup>a</sup> Department of Chemical and Polymer Engineering, UET (Lahore) Faisalabad Campus, Faisalabad, Pakistan

<sup>b</sup> School of Engineering and Design, Brunel University London, Uxbridge, Middlesex, United Kingdom

<sup>c</sup> Thermacore Europe Ltd, Ashington, United Kingdom

Accepted author version posted online: 10 Feb 2014. Published online: 04 Apr 2014.



[Click for updates](#)

To cite this article: Syed W. Ahmad, John S. Lewis, Ryan J. McGlen & Tassos G. Karayiannis (2014) Pool Boiling on Modified Surfaces Using R-123, Heat Transfer Engineering, 35:16-17, 1491-1503, DOI: [10.1080/01457632.2014.889493](https://doi.org/10.1080/01457632.2014.889493)

To link to this article: <http://dx.doi.org/10.1080/01457632.2014.889493>

PLEASE SCROLL DOWN FOR ARTICLE

Taylor & Francis makes every effort to ensure the accuracy of all the information (the "Content") contained in the publications on our platform. Taylor & Francis, our agents, and our licensors make no representations or warranties whatsoever as to the accuracy, completeness, or suitability for any purpose of the Content. Versions of published Taylor & Francis and Routledge Open articles and Taylor & Francis and Routledge Open Select articles posted to institutional or subject repositories or any other third-party website are without warranty from Taylor & Francis of any kind, either expressed or implied, including, but not limited to, warranties of merchantability, fitness for a particular purpose, or non-infringement. Any opinions and views expressed in this article are the opinions and views of the authors, and are not the views of or endorsed by Taylor & Francis. The accuracy of the Content should not be relied upon and should be independently verified with primary sources of information. Taylor & Francis shall not be liable for any losses, actions, claims, proceedings, demands, costs, expenses, damages, and other liabilities whatsoever or howsoever caused arising directly or indirectly in connection with, in relation to or arising out of the use of the Content.

This article may be used for research, teaching, and private study purposes. Terms & Conditions of access and use can be found at <http://www.tandfonline.com/page/terms-and-conditions>

It is essential that you check the license status of any given Open and Open Select article to confirm conditions of access and use.

# Pool Boiling on Modified Surfaces Using R-123

SYED W. AHMAD,<sup>1</sup> JOHN S. LEWIS,<sup>2</sup> RYAN J. MCGLEN,<sup>3</sup>  
and TASSOS G. KARAYIANNIS<sup>2</sup>

<sup>1</sup>Department of Chemical and Polymer Engineering, UET (Lahore) Faisalabad Campus, Faisalabad, Pakistan

<sup>2</sup>School of Engineering and Design, Brunel University London, Uxbridge, Middlesex, United Kingdom

<sup>3</sup>Thermacore Europe Ltd, Ashington, United Kingdom

*Saturated pool boiling of R-123 was investigated for five horizontal copper surfaces modified by different treatments, namely, an emery-polished surface, a fine sandblasted surface, a rough sandblasted surface, an electron beam-enhanced surface, and a sintered surface. Each 40-mm-diameter heating surface formed the upper face of an oxygen-free copper block, electrically heated by embedded cartridge heaters. The experiments were performed from the natural convection regime through nucleate boiling up to the critical heat flux, with both increasing and decreasing heat flux, at 1.01 bar, and additionally at 2 bar and 4 bar for the emery-polished surface. Significant enhancement of heat transfer with increasing surface modification was demonstrated, particularly for the electron beam-enhanced and sintered surfaces. The emery-polished and sandblasted surface results are compared with nucleate boiling correlations and other published data.*

## INTRODUCTION

### Effect of Surface Modification

Surface modification is an effective passive technique for enhancing heat transfer in pool boiling applications. A variety of methods have been investigated, including emery-paper or sandpaper treatments, abrasive blasting, fabricated surface structures, sintered surfaces, and porous coatings.

Gorenflo et al. [1] investigated pool boiling of propane at 4.247 bar on single 8-mm outer diameter (OD) horizontal copper tube surfaces prepared by different treatments—fine sandblasting, medium plus fine sandblasting, and emery grinding—and characterized by  $P_a$  values of 0.27  $\mu\text{m}$ , 0.56  $\mu\text{m}$ , and 0.58  $\mu\text{m}$ , respectively. In nucleate boiling, an increase in  $P_a$  resulted in an increase in the heat transfer coefficient (at constant heat flux). A corresponding decrease of the wall superheat at transition from nucleate boiling to free convection was attributed to the increasing size of the largest surface cavities. Jones et al. [2] examined the effect of surface roughness on pool boiling of

FC-77 and water at atmospheric pressure. Ram-type electrical discharge machining (EDM) was used to prepare 25 mm  $\times$  25 mm aluminium test surfaces with average surface roughness values  $R_a = 1.08 \mu\text{m}$ , 2.22  $\mu\text{m}$ , 5.89  $\mu\text{m}$ , and 10  $\mu\text{m}$ . Polished surfaces with  $R_a$  values of 0.027  $\mu\text{m}$  and 0.038  $\mu\text{m}$  were made for comparison purposes. For FC-77, the heat transfer coefficient (at 100 kW/m<sup>2</sup>) increased continuously with surface roughness by between 2.4 and 3 times that for a smooth surface with  $R_a = 0.027 \mu\text{m}$ . For water, the trend with roughness was less clear and the enhancement was between 1.5 and 1.8 times that for a smooth surface with  $R_a = 0.038 \mu\text{m}$  at the same heat flux. The different behavior for water and FC-77 was attributed to differences in the wetting characteristics of the two liquids and the cavity size distributions of the surfaces.

Kim et al. [3] studied the pool boiling characteristics of treated surfaces, including the effects of subcooling and surface orientation, using the dielectric liquid PF5060 and 20 mm  $\times$  20 mm copper test surfaces. Four different surfaces were tested: a plain surface, a sanded surface, a microfinned surface, and a microporous coated surface. The sanded surface was prepared using grade 80 sandpaper and had an average roughness height of 1.546  $\mu\text{m}$ . For saturated conditions and horizontal orientation, the sanded surface achieved a wall superheat reduction of 43% at 120 kW/m<sup>2</sup> compared to that measured for the plain surface. McGillis et al. [4] obtained experimental data showing the effect of surface finish on pool boiling of water at a

© Syed W. Ahmad, John S. Lewis, Ryan J. McGlen, and Tassos G. Karayiannis

Address correspondence to Professor Tassos G. Karayiannis, School of Engineering and Design, Brunel University London, Uxbridge, Middlesex, UB8 3PH, United Kingdom. E-mail: tassos.karayiannis@brunel.ac.uk

subatmospheric pressure of 9 kPa on three flat copper surfaces. For a constant wall superheat of 25 K, the heat flux increased by about 100% when the root mean square (rms) surface roughness increased from 0.16  $\mu\text{m}$  to 5.72  $\mu\text{m}$ .

McGillis et al. [4] conducted parametric experiments to determine the effects of fin geometry for low-pressure pool boiling of water on rectangular fin arrays at 9 kPa. The fin arrays were machined on 12.7-mm square copper test sections, with fin lengths from 0 to 10.2 mm, fin gaps from 0.3 mm to 3.58 mm, and nominal fin widths of 1.8 mm and 3.6 mm. All the finned surfaces reduced wall superheat and extended the nucleate boiling range compared to smooth surface. However, based on the evidence for fins of 1.8 mm nominal width, additional increase in the base heat flux was fairly marginal for fin lengths greater than 2.54 mm. Smaller fin gaps were found to lead to greater heat transfer enhancement. For example, at 60  $\text{kW/m}^2$ , a fin gap of 0.3 mm resulted in the wall superheat decreasing by 72% compared to a flat surface, whereas for a fin gap of 3.58 mm the decrease in wall superheat was only 28%. No significant influence of fin width on heat transfer rates was reported.

Yu and Lu [5] investigated the heat transfer performance of rectangular fin arrays for saturated pool boiling of FC-72 at 1 atm. The EDM process was used to manufacture  $7 \times 7$ ,  $5 \times 5$ , and  $4 \times 4$  fin array test surfaces from copper blocks of 10 mm  $\times$  10 mm base area, with fin spacings of 0.5 mm, 1 mm, and 2 mm, respectively. Four different fin lengths (0.5 mm, 1 mm, 2 mm, and 4 mm) were investigated and the thickness of the fins was fixed as 1 mm. In general, the heat transfer rate increased as the fin length increased and the fin spacing decreased, with the maximum value being achieved with the fin array having the narrowest fin gaps (0.5 mm) and the highest fins (4 mm), more than five times that for the reference plain surface. Note that the boiling heat transfer coefficient (based on the total finned surface area) was found to be approximately independent of fin length at low heat flux. However, at moderate and high heat flux values, the heat transfer coefficient decreased as the fin length was increased at constant wall superheat.

The microfinned surface tested by Kim et al. [3] was fabricated by etching a copper test block to produce microfins of 100  $\mu\text{m} \times 100 \mu\text{m}$  square cross section with a height of 50  $\mu\text{m}$ . The spacing between the fins was 200  $\mu\text{m}$  and the increase in heat transfer area was 43.6% compared to the original plain surface. Their PF5060 pool boiling curves show that for a heat flux of 120  $\text{kW/m}^2$  the wall superheat for the microfinned surface was 47% lower than for a plain surface.

Surface enhancement techniques for pool boiling include porous microstructures formed by sintered metallic layers and porous coatings. Scurlock [6] presented experimental results for saturated pool boiling of liquid nitrogen and refrigerant R-12 on surfaces with porous aluminum/silicon coatings. The surfaces were manufactured by plasma spraying a mixture of aluminum powder with 10% silicon and polyester on to 50 mm  $\times$  50 mm aluminum plates, which were subsequently heated in air at 500°C for 2 hr to evaporate the polyester. Six surfaces were prepared with coating thicknesses between 0.13 mm and

1.32 mm. For the 0.13-mm-thick coating and a heat flux of 13  $\text{kW/m}^2$ , the wall superheat was found to decrease compared to that for a smooth surface, by approximately 90% for LN<sub>2</sub> and 85% for R-12. The optimum coating thickness for maximum heat transfer coefficient was found to be 0.38 mm for LN<sub>2</sub> and 0.25 mm for R-12. Rainey and You [7] investigated the effect of microporous coated surfaces on pool boiling of saturated FC-72 at atmospheric pressure. Copper test surfaces, 20 mm  $\times$  20 mm and 50 mm  $\times$  50 mm, were coated using a mixture of diamond particles, Omegabond 101, and methyl ethyl ketone (MEK), known as DOM, by drip-coating onto the 20-mm square surface and spray-coating onto the 50-mm square surface. Evaporation of the MEK produced a microporous layer on the surface, approximately 50  $\mu\text{m}$  thick and containing 8–12  $\mu\text{m}$  diamond particles. Heat transfer coefficients for nucleate boiling on the microporous coated surfaces were always augmented by more than 300% compared to those for plain polished surfaces. As previously mentioned, Kim et al. [3] also tested a microporous coated surface for pool boiling of PF5060. The DOM coating applied to the 20-mm square copper test surface contained 4–8  $\mu\text{m}$  diamond particles and was around 45  $\mu\text{m}$  thick. At a heat flux of 120  $\text{kW/m}^2$ , the wall superheat decreased by 66% compared to that for a plain horizontal surface.

### Nucleate Boiling Correlations

Details of some of the correlations proposed to predict heat transfer coefficients in nucleate boiling are set out below. Stephan and Abdelsalam [8] proposed correlations to predict the heat transfer coefficient for water, hydrocarbons, cryogenics, and refrigerants in the nucleate boiling regime. The correlations were based on a regression analysis representing approximately 2800 experimental data points obtained for pool boiling on horizontal surfaces with fully established nucleate boiling under the influence of the gravity field. The pressure range for these data points was  $0.0001 \leq P/P_c \leq 0.97$ . The following correlation developed specifically for refrigerants with  $0.003 \leq P/P_c \leq 0.78$  gave a mean absolute error of 10.6%:

$$h = 207 \frac{k_l}{D_b} \left( \frac{q D_b}{k_l T_s} \right)^{0.745} \left( \frac{\rho_g}{\rho_l} \right)^{0.581} \left( \frac{v_l}{\alpha_l} \right)^{0.533} \quad (1)$$

where the bubble departure diameter  $D_b$  is expressed as

$$D_b = 0.0146\beta \left( \frac{2\sigma}{g(\rho_l - \rho_g)} \right)^{0.5} \quad (2)$$

and the bubble contact angle  $\beta$  was taken as 35° for refrigerants. A mean surface roughness  $R_{p,\text{old}} = 1 \mu\text{m}$  was assumed, where  $R_{p,\text{old}}$  is an older roughness measure defined by the superseded standard DIN 4272:1960 and equal to  $R_a/0.4$  according to Gorenflo et al. [1]. Stephan and Abdelsalam recommended that, to a first approximation, surface roughness may be accounted for by multiplying Eq. (1) by a factor  $R_{p,\text{old}}^{0.133}$ , for  $0.1 \leq R_{p,\text{old}} \leq 10 \mu\text{m}$ .

Cooper [9] developed the following simple correlation for predicting the heat transfer coefficient for nucleate boiling (in  $\text{W}/\text{m}^2\text{-K}$ ) based on the reduced pressure, the heat flux (in  $\text{W}/\text{m}^2$ ), and the surface roughness (in  $\mu\text{m}$ ):

$$h = C(q)^{0.67} M^{-0.5} P_r^n (-\log_{10} P_r)^{-0.55} \quad (3)$$

and the constant was given as  $C = 55$ , but with the suggestion that this value should be replaced by  $C = 95$  for horizontal copper cylinders. The exponent  $n$  is given by

$$n = 0.12 - 0.2 \log_{10} R_{p,old} \quad (4)$$

A comprehensive correlation for predicting pool boiling heat transfer coefficients was suggested by Gorenflo and Kenning [10] in the form

$$\frac{h}{h_{0,ref}} = F_q F_{P_r} F_W F_f \quad (5)$$

The four factors on the right-hand side of Eq. (5) are functions of the heat flux, the reduced pressure, the heating surface, and the fluid properties, respectively, defined as

$$F_q = \left(\frac{q}{q_o}\right)^n \quad (6)$$

where  $q_o = 20 \text{ kW}/\text{m}^2$  and  $n$  is given by

$$n = 0.95 - 0.3 P_r^{0.3} \quad (7)$$

$$F_{P_r} = 0.7 P_r^{0.2} + 4 P_r + \frac{1.4 P_r}{1 - P_r} \quad (8)$$

$$F_W = F_{WR} F_{WM} \quad (9)$$

where

$$F_{WR} = \left(\frac{R_a}{R_{ao}}\right)^{\frac{2}{15}} \quad (10)$$

with the reference surface roughness  $R_{ao} = 0.4 \mu\text{m}$ ,

$$F_{WM} = \left(\frac{k c_p \rho}{(k c_p \rho)_{copper}}\right)^{0.25} \quad (11)$$

and

$$F_f = \left(\frac{P_f}{P_{f,ref}}\right)^{0.6} \quad (12)$$

The fluid parameter  $P_f$  in equation (12) is defined as

$$P_f = \frac{\left(\frac{dP}{dT}\right)_s}{\sigma} \quad (13)$$

where  $(dP/dT)_s$ , the slope of the vapor pressure curve, and  $\sigma$  are both at a reference pressure  $P_r = 0.1$ . Values of  $P_f$ , in  $(\mu\text{m K})^{-1}$ , are tabulated by Gorenflo and Kenning [10] for a large number of fluids. The reference fluid values are  $h_{0,ref} = 3.58 \text{ kW}/\text{m}^2\text{-K}$  and  $P_{f,ref} = 1.0 (\mu\text{m K})^{-1}$ .

Jung et al. [11] developed a correlation to predict pool boiling heat transfer coefficients for pure halogenated refrigerants

by modifying the correlation of Stephan and Abdelsalam [8]. Based on a regression analysis of their experimental data for halogenated refrigerants, they suggested that the power on the heat flux term in Eq. (1) is a function of fluid properties and therefore has a unique value for each refrigerant. The new correlation is as follows:

$$h = 10 \frac{k_l}{D_b} \left(\frac{q D_b}{k_l T_s}\right)^{c_1} P_r^{0.1} (1 - T_r)^{-1.4} \left(\frac{\nu_l}{\alpha_l}\right)^{-0.25} \quad (14)$$

where

$$c_1 = 0.855 \left(\frac{\rho_g}{\rho_l}\right)^{0.309} P_r^{-0.437} \quad (15)$$

and  $D_b$  is given by Eq. (2). Equation (15) fitted the data of Jung et al. with a mean deviation of less than 7%.

Shekrladze [12] presented a correlation for predicting the Nusselt number in developed nucleate boiling. The effective radius of nucleation cavities was assumed to be the characteristic linear dimension, denoted here as  $r_o$ . For commercial heating surfaces it was suggested that  $r_o$  can be represented by an average value of  $5 \mu\text{m}$ . The Shekrladze [12] correlation is as follows:

$$\text{Nu} = \frac{h r_o}{k_l} = 0.88 \times 10^{-2} K^{0.7} \text{Re}_s^{0.25} \quad (16)$$

where

$$K = \frac{q r_o^2 \rho_g h_{lg}}{\sigma k_l T_s} \quad (17)$$

and

$$\text{Re}_s = \frac{c_p T_s \sigma \rho_l}{h_{lg}^{\frac{3}{2}} \rho_g^2 \nu} \quad (18)$$

Yagov [13] proposed a correlation on the basis of boiling fluid properties as follows:

$$q = 3.43 \times 10^{-4} k_l^2 \Delta T^3 \left[1 + \frac{h_{lg} \Delta T}{2 R T_s^2}\right] \times (1 + \sqrt{1 + 800B} + 400B) \quad (19)$$

where

$$B = \frac{h_{lg} (\nu_l \rho_g)^{\frac{3}{2}}}{\sigma (k_l T_s)^{\frac{1}{2}}} \quad (20)$$

Rohsenow [14] developed, much earlier, the following correlation for nucleate boiling of liquids other than water:

$$\frac{c_{pl} \Delta T}{h_{lg}} = C_{sf} \left[\frac{q}{h_{lg} \mu_l} \left(\frac{\sigma}{g(\rho_l - \rho_g)}\right)^{\frac{1}{2}}\right]^{0.33} \left[\frac{c_{pl} \mu_l}{k_l}\right]^{1.7} \quad (21)$$

Jabardo et al. [15] reevaluated the exponents and the leading coefficient  $C_{sf}$  in the Rohsenow correlation using experimental data for refrigerants. Modified exponents were determined

as 0.21 and 1.03, replacing the values 0.33 and 1.7, respectively, in Eq. (21).  $C_{sf}$  was expressed as a function of average surface roughness, fluid/surface material combination, and reduced pressure as follows:

$$C_{sf} = C [(a \ln R_a - b) P_r - c \ln R_a + d] \quad (22)$$

For R-123 and copper the following values were found:  $C = 1$ ,  $a = 0.0077$ ,  $b = 0.0258$ ,  $c = 0.0036$ , and  $d = 0.0138$ .

In this paper, experimental data are presented for saturated pool boiling of refrigerant R-123 on five different copper heating surfaces, namely, emery-polished, fine sandblasted, rough sandblasted, electron beam (EB) enhanced, and sintered surfaces. The data are compared with pool boiling correlations and experimental results published in the literature.

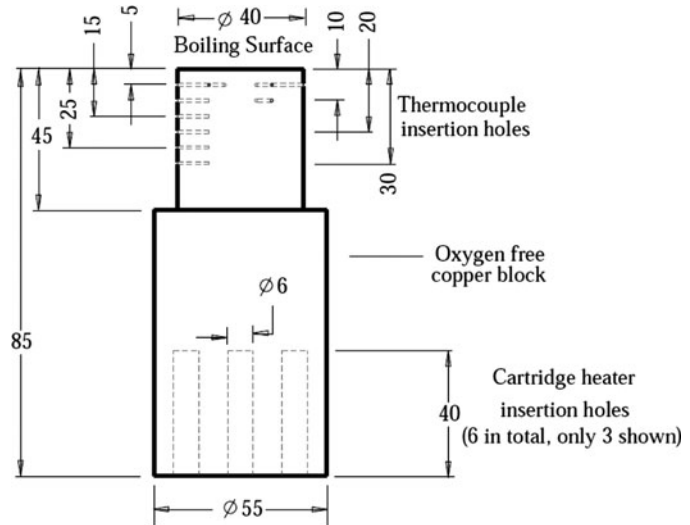


Figure 2 Schematic diagram of the heater block.

30 mm below the boiling surface in holes of 1 mm diameter and 10 mm deep. The heater block was heavily insulated by a thick PTFE sleeve. The temperature in the boiling chamber was measured by three Type K thermocouples, two placed in the liquid region and one in the vapor region.

A pressure gauge and a pressure transducer were connected at the top of the chamber to monitor the pressure. To maintain saturated conditions within the chamber and to reduce heat loss an electric heater tape was wrapped around the chamber and nitrile foam rubber insulation was applied to a thickness of approximately 25 mm.

## EXPERIMENTAL PROCEDURE AND DATA REDUCTION

The boiling chamber and condenser were initially filled with  $N_2$  at 2.5 bar pressure to carry out a leakage test. Once the system was leak free, R-123 was admitted to the boiling chamber in vapor form. The refrigerant was filled to 80 mm above the boiling surface. The fluid was then boiled at a moderate heat flux for 30 min to remove any noncondensable gases, which were vented through a valve above the condenser. Measurements were recorded after the system reached a steady state. Tests were performed at 1.01 bar pressure for all the surfaces, for both increasing and decreasing heat flux, from the natural convection regime through nucleate boiling up to the critical heat flux. The effect of pressure was investigated for the emery-polished surface by conducting additional tests at 2 bar and 4 bar.

The temperature gradient in the heater block and the temperature of the boiling surface were determined using the temperatures recorded at the six thermocouple positions shown in Figure 2; see Ahmad [16]. The heat flux was then calculated

## EXPERIMENTAL SETUP

The experimental facility, shown schematically in Figure 1, consisted of the following main components: (a) the boiling chamber housing the heater block, (b) a R-123 condenser, (c) a cooling water loop, and (d) a R-134a cooling unit. Electrical power supply and measurement equipment completed the experimental setup. Saturated pool boiling of R-123 was carried out in the boiling chamber. The system operated as a two-phase thermosyphon. R-123 vapor produced in the boiling chamber was condensed in a water-cooled condenser and the condensate returned to the chamber via a filter/dryer. The cooling water used in the condenser was recirculated and chilled in a heat exchanger using a R-134a vapor compression refrigeration unit. The boiling chamber was a vertical stainless steel 304 cylinder, 220 mm in diameter and 300 mm in height. Two circular glass windows, 140 mm in diameter, were mounted in the sides of the chamber in order to visualize the boiling process. Each boiling surface investigated was formed by the 40-mm upper face of a cylindrical heater block manufactured from oxygen-free copper, as illustrated in Figure 2. Six 250-W cartridge heaters were installed in the lower end of the heater block. The power supplied to the heaters was regulated using a variable transformer and measured by a power meter. Temperatures in the heater block were measured using six Type K thermocouples of 0.5 mm diameter located 5 mm, 10 mm, 15 mm, 20 mm, 25 mm, and

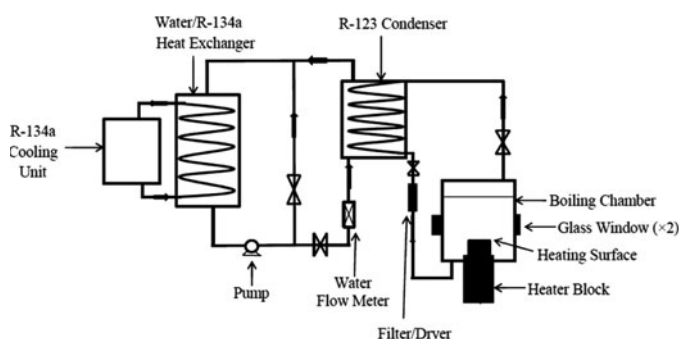


Figure 1 Schematic diagram of the experimental facility.

**Table 1** Properties of saturated R-123 extracted from EES software

| Property                                  | $P = 1.01$ |             |             |
|---|------------|-------------|-------------|
|   | bar        | $P = 2$ bar | $P = 4$ bar |
| Saturation temperature (K)                | 300.8      | 321.2       | 345.3       |
| Density of vapor ( $\text{kg/m}^3$ )      | 6.455      | 12.31       | 23.98       |
| Density of liquid ( $\text{kg/m}^3$ )     | 1457       | 1403        | 1335        |
| Specific enthalpy of vaporization (J/kg)  | 170600     | 161600      | 149700      |
| Specific heat capacity of liquid (J/kg-K) | 1039       | 1070        | 1112        |
| Surface tension (N/m)                     | 0.01486    | 0.01251     | 0.00982     |
| Dynamic viscosity of liquid (kg/m-s)      | 0.00041    | 0.000323    | 0.00025     |
| Thermal conductivity of liquid (W/m-K)    | 0.07651    | 0.0714      | 0.0654      |

using

$$q = k_{cu} \left( \frac{dT}{dy} \right)_{y=0} \quad (23)$$

assuming heat flow in the copper block to be one-dimensional; see Ahmad et al. [17]. The heat transfer coefficient at the boiling surface was calculated as

$$h = \frac{k_{cu}}{(T_s - T_w)} \left( \frac{dT}{dy} \right)_{y=0} \quad (24)$$

All the thermocouples were calibrated against a precision thermometer (F250 MKII, Automatic System Laboratories) and the pressure transducer was calibrated against a dead weight tester. The uncertainty for the pressure transducer measurements was  $\pm 0.5$  kPa, and for the thermocouple measurements was  $\pm 0.2$  K. The location error of the thermocouples was estimated to be  $\pm 0.05$  mm. The boiling surface temperature  $T_w$  was determined with a maximum uncertainty of 0.22 K as the intercept value of a linear regression line fitted through the temperatures measured within the copper block; see Ahmad [16] for further details.

The uncertainty in the heat flux  $q$  was calculated as follows:

$$\left( \frac{U_q}{q} \right)^2 = \left( \frac{U_{k_{cu}}}{k_{cu}} \right)^2 + \left( \frac{U_m}{m} \right)^2 \quad (25)$$

where  $m$  denotes the slope of the linear regression line that gives the temperature gradient  $dT/dy$  in the heater block. The propagation of uncertainties in  $h$  was determined using Eq. (26); see Coleman and Steele [18].

$$\left( \frac{U_h}{h} \right)^2 = \left( \frac{U_q}{q} \right)^2 + \left( \frac{U_{T_w}}{T_w - T_s} \right)^2 + \left( \frac{U_{T_s}}{T_w - T_s} \right)^2 \quad (26)$$

The uncertainty in the heat flux was between 2 and 4% and for heat transfer coefficient was between 2.5 and 5% in the nucleate boiling regime. All properties of R-123 were found using the EES (Engineering Equation Solver) software; see Table 1.

### SURFACE PREPARATION AND CHARACTERIZATION

According to Piore et al. [19], the effect of surface characteristics on boiling heat transfer rates depends on the thermophys-

ical properties of the surface material, the solid–liquid–vapor interactions, and the surface microgeometry. As discussed in the introduction, surface roughness can be a good indicator of the effect of surface condition on the pool boiling heat transfer coefficient, as found by Gorenflo et al. [1], Jones et al. [2], and Kim et al. [3]. However, beyond that, it is worth noting that surface microstructure, which refers to the shape, dimensions, and density of pores and cracks, is fundamentally important as it relates to the number of possible nucleation sites (Piore et al. [19]). Therefore, conventional surface roughness parameters such as the average roughness  $R_a$  and the root mean square roughness  $R_q$  may not be entirely adequate to represent the surface microstructure and hence the actual behavior of a surface in boiling. Piore et al. [19] pointed out that “for the same value of surface roughness, two extreme cases of microstructure may exist – plateau with peaks and plateau with valleys and cavities.” Thus, the  $R_a$  values, on their own, would not be a good indicator of the comparative boiling performance of these two surfaces. Surface roughness does, however, affect the heat transfer coefficient when the number of active nucleation sites increases as  $R_a$  increases, which can often be the case.

The procedures to prepare the test surfaces used in this study are outlined in the following. All the surfaces were characterized using an ultrasonic stylus instrument at Kassel University as described by Luke [20]. Two-dimensional surface profiles were obtained for each surface; see Figures 3–7. Average values were reported for the primary profile amplitude parameters  $P_a$  and  $P_q$ , evaluated on the basis of the unfiltered primary profile. The parameter  $P_a$  is defined in the BS EN ISO 4287:1998 standard as the arithmetic mean value of the absolute values of the profile deviations from the mean line within a sampling length and is expressed by

$$P_a = \frac{1}{l_p} \int_0^{l_p} |Z(x)| dx \quad (27)$$

where  $l_p$  is the sampling length of the primary profile. In a similar way,  $P_q$  is defined as the root mean square value of the profile deviations from the mean line within a sampling length and is given by

$$P_q = \sqrt{\frac{1}{l_p} \int_0^{l_p} Z^2(x) dx} \quad (28)$$

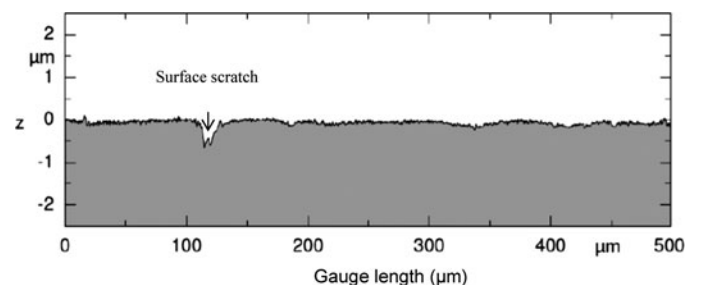


**Figure 3** Two-dimensional profile for the emery-polished surface.

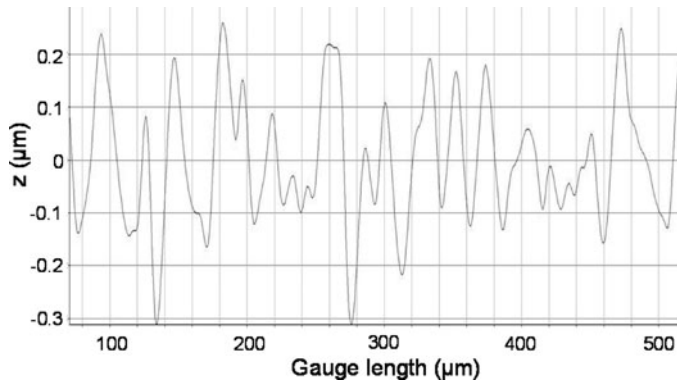


Figure 4 Two-dimensional profile for the fine sandblasted surface.

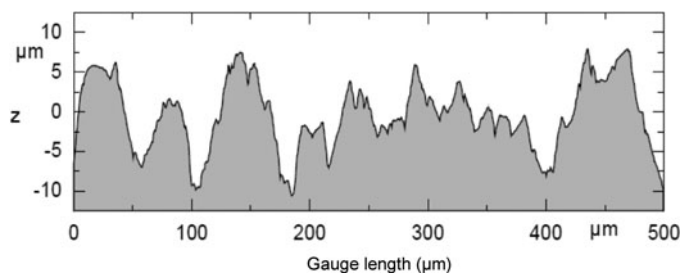


Figure 5 Two-dimensional profile for the rough sandblasted surface.

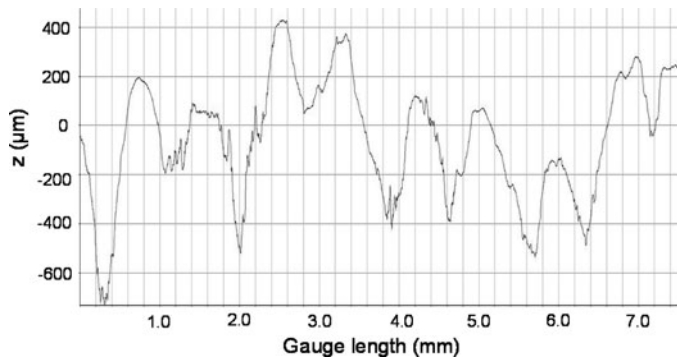


Figure 6 Two-dimensional profile for the EB enhanced surface.

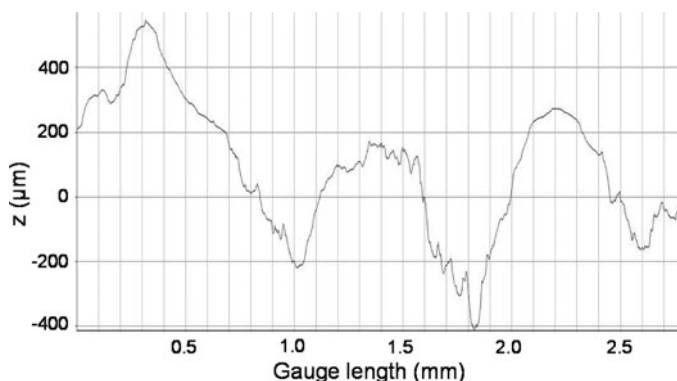


Figure 7 Two-dimensional profile for the sintered surface.

In this work,  $P_a$  was substituted for the average surface roughness  $R_a$  in evaluating any nucleate boiling heat transfer correlation equation involving the surface roughness. The average surface roughness  $R_a$  is evaluated in the same manner as  $P_a$ , but is based instead on a roughness profile. The roughness profile is derived from the primary profile by suppressing the long wave component using a profile filter with a cutoff wavelength  $\lambda_c$  that defines the intersection of the roughness and waviness components present in a surface; see BS EN ISO 16610-21: 2012 for more details.

#### *Emery-Polished Surface*

The surface was polished with emery paper P1200. It was placed on the emery paper under its own weight of 24.5 N. The block was moved on the emery paper from front to back and then sideways, 50 times in each direction. After every 50 movements the emery paper was renewed. Compressed nitrogen was then blown over the surface to remove any fine particles. The values of  $P_a = 0.044 \mu\text{m}$  and  $P_q = 0.069 \mu\text{m}$  were obtained for the emery-polished surface.

#### *Fine Sandblasted Surface*

The surface was first carefully polished and then sandblasted with brown aluminum oxide (grit size 120–220  $\mu\text{m}$ ) in a standard sandblasting cabinet, as discussed in Luke [20]. During sandblasting the nozzle to surface distance was kept at 60 mm and the operating pressure was 3.5 bar. The  $P_a$  value for this fine sandblasted surface was  $0.0997 \mu\text{m}$  and the  $P_q$  value was  $0.1211 \mu\text{m}$ .

#### *Rough Sandblasted Surface*

The surface was prepared using the same procedure as used for the fine sandblasted surface, but with a coarser abrasive blasting material. Brown aluminum oxide (grit size 300–425  $\mu\text{m}$ ) was used. The rough sandblasted surface was found to have a surface parameter value  $P_a = 3.52 \mu\text{m}$  and  $P_q = 4.43 \mu\text{m}$ .

#### *Electron Beam (EB)-Enhanced Surface*

This enhanced surface was prepared at TWI Cambridge using an electron beam surface modification technology known as Surf-Sculpt. In this process the electron beam is moved across the surface by a programmable system, causing melting and displacement of surface material to form an array of protrusions. The process is discussed in detail by Buxton et al. [21]. The values of  $P_a = 200 \mu\text{m}$  and  $P_q = 243 \mu\text{m}$  were determined for the EB-enhanced surface.

### Sintered Surface

The sintering procedure was carried out at Thermacore Europe. The sintered surface was created by sintering copper particles directly onto the upper face of the heater block. To produce the required thickness of particles a custom-designed mandrel was clamped to the block, forming a chamber with a uniform depth of 0.5 mm. Copper powder was inserted into the chamber and vibrated to ensure the particles were close-packed. The assembly was heated in an inert atmosphere to just below the melting point of copper, allowing the particles to fuse together and to the surface of the heater block as a porous metal layer. To enable the material to fuse, a secondary gas was used that fluxes with the powder to remove the oxide layer. The values  $P_a = 144 \mu\text{m}$  and  $P_q = 181 \mu\text{m}$  were found for the sintered surface.

## RESULTS AND DISCUSSION

Experimental data were collected for both increasing and decreasing heat flux for all of the surfaces tested. Only results for decreasing heat flux are presented in this paper. Hysteresis was only observed for the rough sandblasted surface and the EB enhanced surface. The repeatability of the results was routinely checked throughout the experiments. It was found that they were repeatable within the experimental error.

### Effect of Surface Roughness

Figure 8 presents experimental data obtained in this study and earlier work by Ahmad et al. [17] and Ahmad et al. [22] for pool boiling of R-123 at 1 bar pressure on copper surfaces prepared using different methods, namely, emery polishing, fine and rough sandblasting, electron-beam surface enhancement, and sintering. The spread of the boiling curves in Figure 8 demonstrates that surface modification has an appreciable effect

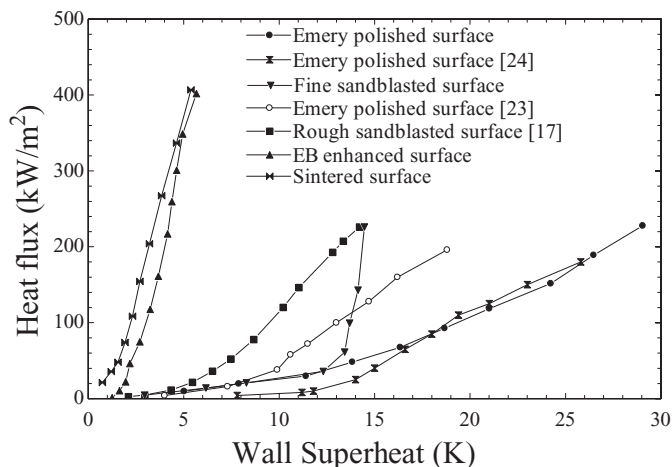


Figure 8 Boiling curves for the modified surfaces, at  $P = 1.01$  bar.

on the variation of heat flux with wall superheat. Experimental results reported by Zaghoudi and Lallemand [23] and Hristov et al. [24] for pool boiling of R-123 at 1 bar on emery treated copper surfaces are also plotted in Figure 8 for comparison.

The results obtained for the emery-polished surface with  $P_a = 0.044 \mu\text{m}$  are in reasonably good agreement with the measurements of Hristov et al. [24], who utilized an earlier version of the apparatus shown in Figure 1 at Brunel University and a boiling surface polished using P1200 emery paper followed by an ultrafine abrasive paper. In contrast, the results of Zaghoudi and Lallemand [23] exhibit an earlier rise of heat flux with wall superheat for a surface prepared using number 600 emery paper. It should be noted that number 600 emery paper is much coarser than grade P1200 and therefore would be expected to produce larger cavities and deeper peak-to-valley roughness in the surface, with greater potential for bubble formation at lower wall superheats. Beyond this, it is difficult to compare the emery-polished surface results obtained by the present authors and Hristov et al. [24] and those of Zaghoudi and Lallemand [23] because surface roughness was not quantified in the latter two studies.

The experimental results shown in Figure 8 for the two sandblasted boiling surfaces are characterized by different values of the standardized surface parameter:  $P_a = 0.099 \mu\text{m}$  for the fine sandblasted surface and  $P_a = 3.5 \mu\text{m}$  for the rough sandblasted surface. As heat flux and wall superheat increase, the fine sandblasted surface data are initially in line with the curve for the emery-polished surface when natural convection is the principal heat transfer mode. At a wall superheat slightly above 12 K the fine sandblasted results diverge sharply upward with the onset of nucleate boiling. This enhancement of boiling heat transfer is consistent with the presence of larger cavities on the rougher surface: that is,  $P_a = 0.099 \mu\text{m}$ , compared to  $0.044 \mu\text{m}$  for the polished surface. It should be mentioned that the roughness value reported here for the emery-polished surface may be slightly high due to surface scratches within the gauge length over which  $P_a$  was evaluated, as indicated in Figure 3.

In the case of the rough sandblasted surface ( $P_a = 3.5 \mu\text{m}$ ) the boiling curve is further shifted to the left in Figure 8, compared with the curves for the fine sandblasted and emery-polished surfaces. This pattern illustrates a progressive decrease, with increase of the surface roughness, of the wall superheat needed to dissipate a given heat flux by nucleate pool boiling on these surfaces. Inspection of the two-dimensional surface profiles in Figures 4 and 5 shows that the microstructure of the rough sandblasted test surface had much deeper valleys, higher peaks, and a wider distribution of cavity sizes than the fine sandblasted test surface. Hence, the rough sandblasted surface microstructure would be more effective, both in a vapor trapping role and in promoting bubble formation over a range of wall superheats.

The EB-enhanced surface and the sintered surface both achieved a large improvement in heat transfer compared to the conventional emery-polished and sandblasted surfaces, as evidenced by their much steeper boiling curves in Figure 8. Application of the EB surface modification process causes the



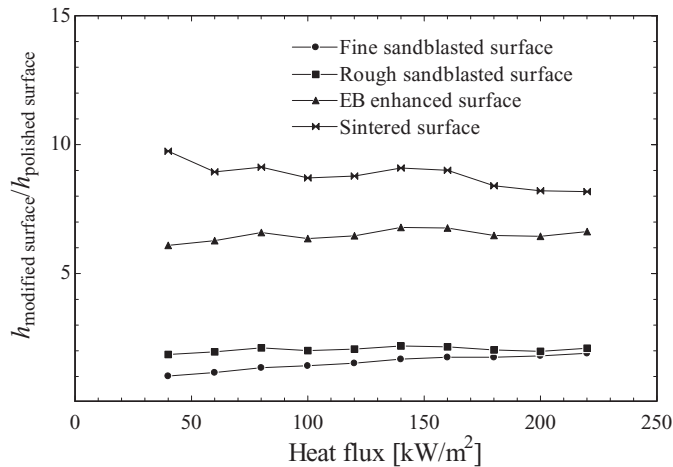


**Figure 9** Augmentation of heat transfer coefficient due to surface modification.

growth of a pattern of protrusions above the original surface level, accompanied by associated cavities in the substrate. This macrostructure is reflected by the large value of the standardized surface parameter,  $P_a = 200 \mu\text{m}$ , measured for the EB-enhanced surface, significantly larger than the  $P_a$  values determined for the other surfaces tested. The effectiveness of the cavities formed by the EB surface enhancement technique in trapping vapor is believed to be the primary reason for the large observed augmentation of heat transfer in nucleate boiling.

In addition, the increase in the heat transfer surface area provided by the protrusions may be a secondary factor contributing to an increase in the base heat flux. The strongest influence of surface modification on pool boiling heat transfer is displayed by the sintered surface results shown in Figure 8, although the surface  $P_a = 144 \mu\text{m}$  was smaller than for the EB enhanced surface. The sintering process forms a porous metallic (copper) structure on the heater block surface of assumed uniform porosity and cavity distribution, providing vapor entrapment volume and a large number of active nucleation sites.

The heat transfer coefficient augmentation can be expressed as the ratio  $h_{\text{modified surface}}/h_{\text{polished surface}}$ . Trend lines of this factor are compared in Figure 9 for heat fluxes up to  $220 \text{ kW/m}^2$ . For the sintered, EB-enhanced, rough sandblasted, and fine sandblasted test surfaces the heat transfer coefficients were found to be augmented by around 9, 6.5, 2, and 1.5 times the value for the emery-polished surface, respectively.

### Comparison With Correlations

Experimental heat transfer coefficients obtained in this study for pool boiling of R-123 on the emery-polished surface, at pressures of 1.01 bar, 2 bar, and 4 bar, are compared with predictions based on published nucleate boiling correlations in Figures 10, 11, and 12, respectively. Similar comparisons are presented in Figures 13 and 14 for the results obtained at 1.01 bar with the fine sandblasted surface and the rough sandblasted surface, respectively. These surfaces cover a range of roughness with

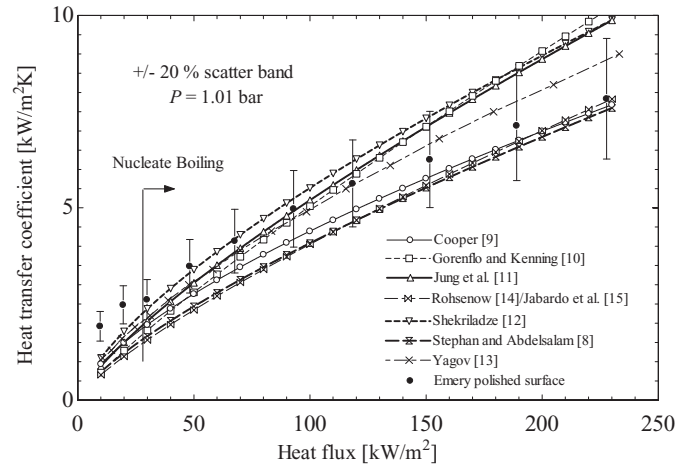


**Figure 10** Comparison of pool boiling results for the emery-polished surface with published correlations, at  $P = 1.01$  bar.

standardized surface parameter values  $P_a = 0.044 \mu\text{m}$  (emery-polished),  $P_a = 0.099 \mu\text{m}$  (fine sandblasted), and  $P_a = 3.5 \mu\text{m}$  (rough sandblasted). As previously mentioned,  $P_a$  values were substituted for the average surface roughness  $R_a$  in prediction calculations, although it is noted that the roughness of the heater surface is not used in all of the correlation equations considered here.

The correlation proposed by Stephan and Abdelsalam [8] for refrigerants, given by Eq. (1), is based on a regression analysis of published data covering a wide range of reduced pressure and includes thermal, transport and wetting properties of the fluid. An average surface roughness  $R_{p,old} = 1 \mu\text{m}$  was assumed in the development of this correlation. It was suggested that Eq. (1) should be multiplied by  $R_{p,old}^{0.133}$  to account for the influence of surface roughness values other than  $1 \mu\text{m}$ . When this factor is applied with the Stephan–Abdelsalam correlation, as plotted in Figure 10, the calculated heat transfer coefficients underpredict the experimental results for the emery-polished surface at  $P = 1.01$  bar, only falling within the  $\pm 20\%$  error band at higher heat

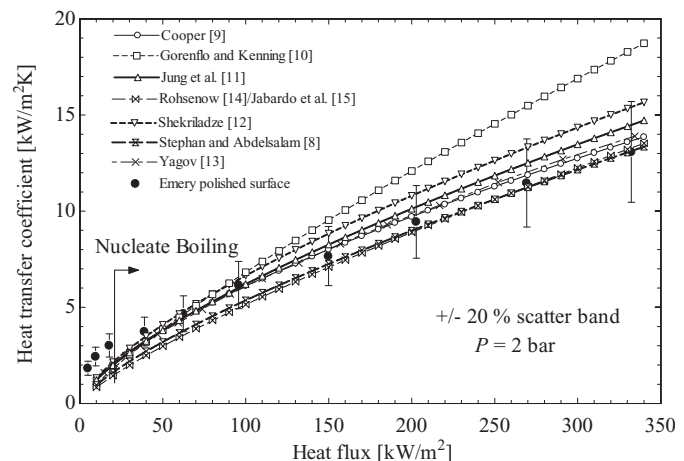


**Figure 11** Comparison of pool boiling results for the emery-polished surface with published correlations, at  $P = 2$  bar.

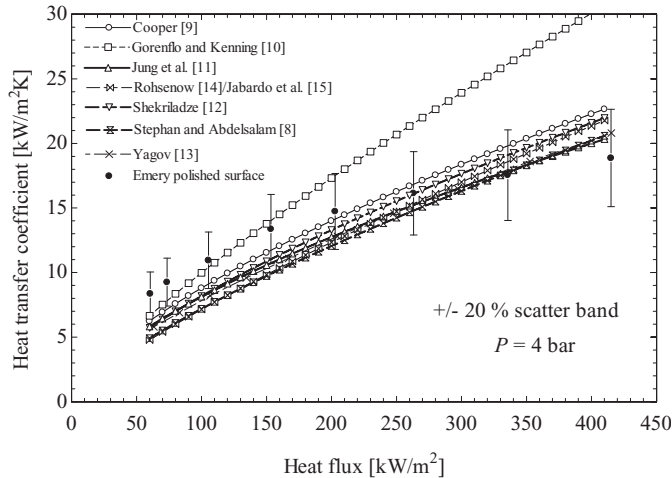


**Figure 12** Comparison of pool boiling results for the emery-polished surface with published correlations, at  $P = 4$  bar.

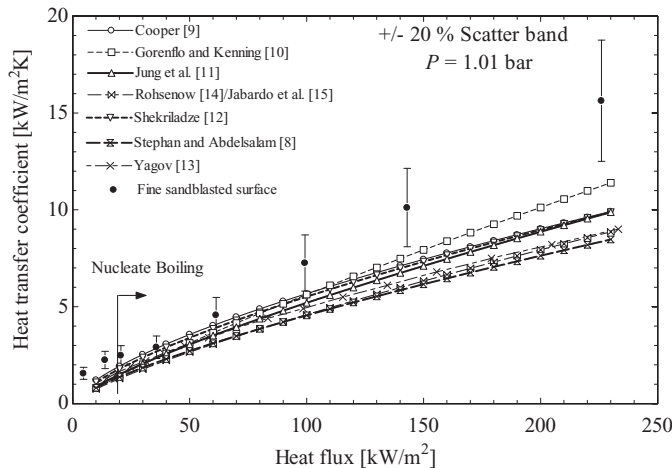


**Figure 13** Comparison of pool boiling results for the fine sandblasted surface with published correlations, at  $P = 1.01$  bar.

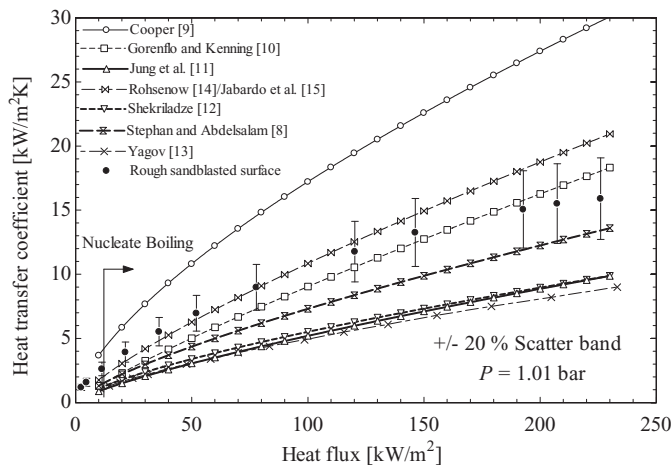


**Figure 14** Comparison of pool boiling results for the rough sandblasted surface with published correlations,  $P = 1.01$  bar.

fluxes. If the surface roughness factor is not included, the predictions (not shown) are within  $\pm 20\%$  of the experimental data in the mid-to-low heat flux range, but are too high at high heat fluxes and too low at low heat fluxes. In the simple correlation developed by Cooper [9], the properties of the boiling fluid are represented in terms of the reduced pressure  $P_r$  and the molecular mass  $M$  only. The heater surface roughness measure  $R_{p,old}$  is included in an exponent on  $P_r$ . The Cooper correlation predicted line in Figure 10, calculated using Eq. (3) with  $C = 95$ , exhibits closer agreement with the  $P = 1.01$  bar experimental results than that of the Stephan–Abdelsalam correlation and remains within the  $\pm 20\%$  error band apart from at the lowest heat flux values. The Jung et al. [11] correlation for halogenated refrigerants is a modified form of the Stephan and Abdelsalam [8] correlation and, following Cooper [9], introduces the reduced properties  $P_r$  and  $T_r$ . However, their equation does not include any term to account for the heater surface condition. Predicted values calculated with the Jung et al. correlation are within  $\pm 20\%$  of the polished surface experimental data for  $P = 1.01$  bar, except at the extremes of the heat flux range.

Heat transfer coefficients predicted from the correlations and the experimental results for the emery-polished surface, at test pressures of 2 bar and 4 bar, are compared in Figures 11 and 12, respectively. It is evident that the correlations discussed earlier, due to Stephan and Abdelsalam [8], Cooper [9], and Jung et al. [11], show better agreement with the data at  $P = 2$  bar than with data obtained at the 1.01 bar and 4 bar conditions. The heat transfer prediction equation developed by Yagov [13] is based on an approximate theoretical model of nucleate boiling and includes empirically determined constants and the boiling fluid properties. Predictions made with this equation show close agreement with the experimental data for the emery-polished surface at 1.01 bar and 2 bar, but less good agreement at 4 bar; see Figures 10, 11, and 12.

The calculation method of Gorenflo and Kenning [10] involves nondimensional functions representing the relative influences of heat flux, reduced pressure, fluid properties, and heating surface roughness and material properties on the heat transfer coefficient relative to that for a fictitious reference fluid. For  $P = 1.01$  bar, the predicted coefficients are within the range of values given by the other correlations, as shown in Figure 10. However, at 2 bar and 4 bar, the predicted values only agree at low heat fluxes, but then deviate increasingly as the heat flux increases, as can be seen in Figures 11 and 12. This behavior is presently unexplained and requires further investigation.

Shekrladze [12] developed a nucleate boiling correlation with the average effective radius at the mouth of nucleation cavities as the characteristic linear size. As mentioned earlier, Shekrladze [12] suggested using a value  $r_o = 5 \mu\text{m}$  as typical of commercial surfaces. Since  $r_o$  was unknown for the emery-polished and sandblasted surfaces tested in this work, a constant value of  $5 \mu\text{m}$  was used in order to evaluate Eq. (16). Nevertheless, the predicted heat transfer coefficients are mostly within  $\pm 20\%$  of the experimental results for the emery-polished surface at all pressures, except at low heat fluxes.

**Table 2** Mean absolute error (MAE) between the predicted and experimental heat transfer coefficient values for the emery-polished surface at different pressures

| Correlation                       | MAE (%)<br>at 1.01 bar | MAE (%)<br>at 2 bar | MAE (%)<br>at 4 bar |
|-----------------------------------|------------------------|---------------------|---------------------|
| Cooper [9]                        | 13.8                   | 5.4                 | 14.8                |
| Stephan and Abdelsalam [8]        | 19.7                   | 10.8                | 21.7                |
| Jung et al. [11]                  | 13.5                   | 8.2                 | 16.2                |
| Rohsenow [14]/Jabardo et al. [15] | 20.1                   | 13.4                | 22.7                |
| Yagov [13]                        | 9.0                    | 6.5                 | 17.9                |
| Gorenflo and Kenning [10]         | 17.3                   | 21.9                | 26.4                |
| Shekriladze [12]                  | 11.9                   | 11.4                | 16.9                |

Jabardo et al. [15] employed curve fits of experimental data for refrigerants (including R-123) to modify the exponents and the surface–fluid coefficient  $C_{sf}$  in the original Rohsenow [14] nucleate boiling correlation. An expression, Eq. (22), was developed for calculating  $C_{sf}$  as a function of surface roughness and reduced pressure. Predictions made using the modified correlation are comparable with those of the Stephan and Abdelsalam [8] correlation (including the surface roughness factor).

Deviations of the predicted heat transfer coefficient values from the experimental data for the emery-polished surface are presented in Table 2 in the form of the mean absolute error (MAE) expressed in percentage terms as

$$\text{MAE} = \frac{1}{N} \sum_{i=1}^N \frac{|h_{i,exp} - h_{i,pre}|}{h_{i,exp}} \times 100 \quad (29)$$

It should be noted that the MAE values in Table 2 are based on the limited number of experimental data points shown in Figures 10–12. Furthermore, MAE provides an average measure of the deviations between predicted and experimental values, and does not differentiate between overprediction and underprediction. For example, Table 2 shows roughly equal MAE values for the Cooper [9] correlation predictions of 13.8% at 1.01 bar and 14.8% at 4 bar. However, Figure 10 reveals that although the predictions for  $P = 1.01$  bar fall consistently below the experimental results, the  $P = 4$  bar data are overpredicted at high heat flux.

Figures 10–12, and the preceding discussion, relate to the emery-polished surface characterized by a  $P_a$  value of  $0.044 \mu\text{m}$ . It is of interest to examine how the same correlations perform in predicting heat transfer coefficients for the fine and rough sandblasted surfaces. Table 3 lists MAE values comparing the predictions with the experimental data for the sandblasted surfaces. The predictions from the Jung et al. [11], Yagov [13], and Shekriladze [12] correlations for the sandblasted surfaces shown in Figures 13 and 14 are identical to those for the emery-polished surface shown in Figure 10. This is because the conditions (saturated,  $P = 1.01$  bar), and hence fluid properties, were the same in all cases and because surface roughness does not appear in these correlations. Also, a constant value of  $r_o$  was assumed in the Shekriladze correlation.

**Table 3** Mean absolute error (MAE) between the predicted and experimental heat transfer coefficient values for the sandblasted surfaces at 1.01 bar

| Correlation                       | Fine sandblasted<br>surface<br>MAE (%) | Rough sandblasted<br>surface<br>MAE (%) |
|-----------------------------------|--|---|
| Cooper [9]                        | 20.3                                   | 68.1                                    |
| Stephan and Abdelsalam [8]        | 37.8                                   | 28.7                                    |
| Jung et al. [11]                  | 29.6                                   | 49.2                                    |
| Rohsenow [14]/Jabardo et al. [15] | 38.3                                   | 14.6                                    |
| Yagov [13]                        | 30.4                                   | 51.3                                    |
| Gorenflo and Kenning [10]         | 25.7                                   | 17.3                                    |
| Shekriladze [12]                  | 23.4                                   | 46.2                                    |

In the case of the fine sandblasted surface (see Figure 13), all the predictions fall below the experimental data. In Figure 9, the heat transfer coefficient augmentation for the fine sandblasted surface was around 1.5 times that of the emery-polished surface, for an increase in  $P_a$  from  $0.044 \mu\text{m}$  to  $0.099 \mu\text{m}$ , whereas the dependence of  $h$  on surface roughness in the Stephan–Abdelsalam and Gorenflo–Kenning equations follows a weaker  $h \propto R_a^{4/15}$  relationship. Furthermore, it is known that sandblasted surfaces have a uniform granular microstructure with a larger size distribution of cavities, or roughness range, than produced by emery grinding; see Luke [25]. The preceding comparison illustrates that the use of  $R_a$  alone may not be adequate to fully represent the effect of surface condition on pool boiling heat transfer.

The comparison for the rough sandblasted surface ( $P_a = 3.5 \mu\text{m}$ ) in Figure 14 shows large deviations between the predictions and the experimental data, as expected, except for the Jabardo et al. [15] modification of the Rohsenow [14] correlation and the Gorenflo and Kenning [10] correlation.

## CONCLUSIONS

The effects of heater surface modifications on pool boiling in saturated R-123 were investigated experimentally. Boiling curves were established for emery-polished, sandblasted, electron beam enhanced, and sintered surfaces. The following conclusions can be drawn:

1. Surface modification can yield significant enhancement of the heat transfer coefficient. The best performance was achieved by the sintered surface with a heat transfer coefficient approximately nine times that for the emery-polished surface. The corresponding augmentation factors for the EB-enhanced, fine sandblasted, and rough sandblasted surfaces were around 6.5, 2, and 1.5 respectively.
2. The experimental heat transfer coefficients for the emery-polished surface (at 1.01 bar, 2 bar and 4 bar) were compared with predictions from seven different nucleate boiling correlations. Some correlations gave predictions within  $\pm 20\%$  of the experimental results over wide ranges of heat flux

and pressures. Comparison of experimental and predicted coefficients for the sandblasted surfaces (at 1.01 bar) showed much greater disagreement, with general underprediction for the fine sandblasted surface and some large deviations for the rough sandblasted surface.

3. The pool boiling results obtained for the emery-polished surface and two sandblasted surfaces suggest that the effect of different heater surface conditions may not be adequately represented by the dependence of heat transfer coefficient on average surface roughness  $R_a$  assumed in the nucleate boiling correlations. Further work is required to elucidate the influence of surface characteristics on boiling heat transfer.

### FUNDING

The first author was supported by the University of Engineering & Technology Lahore, Pakistan under the Faculty Development Programme. The technical support of Prof. A. Luke of Kassel University and Dr. A. L. Buxton of TWI Cambridge is also acknowledged.

### NOMENCLATURE

|          |  |
|----------|--|
| $A$      | area, $m^2$  |
| $a, b$   | constants in Eq. (22), dimensionless                           |
| $B$      | defined by Eq. (20), dimensionless                             |
| $C$      | constant in Eq. (3, 22), dimensionless                         |
| $c$      | constant in Eq. (22), dimensionless                            |
| $c_1$    | defined by Eq. (15), dimensionless                             |
| $c_p$    | specific heat capacity, $kJ/kg\cdot K$                         |
| $C_{sf}$ | constant in Eq. (21), dimensionless                            |
| $D_b$    | bubble departure diameter, $m$                                 |
| $d$      | constant in Eq. (22), dimensionless                            |
| $f$      | total number of data points, dimensionless                     |
| $F_f$    | function of fluid properties, Eqs. (5) and (12), dimensionless |
| $F_{Pr}$ | function of reduced pressure, Eqs. (5) and (8), dimensionless  |
| $F_q$    | function of heat flux, Eqs. (5) and (6), dimensionless         |
| $F_W$    | function of heater wall, Eqs. (5) and (9), dimensionless       |
| $F_{WR}$ | function of wall roughness, Eqs. (9) and (10), dimensionless   |
| $F_{WM}$ | function of wall material, Eqs. (9) and (11), dimensionless    |
| $g$      | acceleration due to gravity, $m/s^2$                           |
| $h$      | heat transfer coefficient, $kW/m^2\cdot K$                     |
| $h_{lg}$ | specific enthalpy of vaporization, $kJ/kg$                     |
| $K$      | variable in Eqs. (16) and (17), dimensionless                  |
| $k$      | thermal conductivity, $kW/m\cdot K$                            |
| $l_p$    | sampling length of primary profile, $\mu m$                    |
| $M$      | molecular mass, $kg/kmol$                                      |
| $m$      | temperature gradient, $K/m$                                    |
| $Nu$     | Nusselt number, dimensionless                                  |

|             |  |
|-------------|--|
| $n$         | exponent in Eqs. (3) and (6), dimensionless            |
| $P$         | pressure, $bar$  |
| $P_a$       | arithmetic mean deviation of primary profile, $\mu m$  |
| $P_f$       | defined by Eq. (13), $(\mu m\cdot K)^{-1}$             |
| $P_q$       | root mean square deviation of primary profile, $\mu m$ |
| $q$         | heat flux, $kW/m^2$                                    |
| $R$         | specific gas constant, $kJ/kg\cdot K$                  |
| $R_a$       | average surface roughness, $\mu m$                     |
| $R_{p,old}$ | surface roughness defined by DIN 4272:1960, $\mu m$    |
| $Re_s$      | modified Reynolds number, dimensionless                |
| $r_o$       | average cavity radius, $m$                             |
| $T$         | temperature, $K$                                       |
| $U_i$       | uncertainty of $i$ th component                        |
| $x$         | distance along the boiling surface, $m$                |
| $y$         | distance below the boiling surface, $m$                |
| $Z$         | profile deviation from mean line, $\mu m$              |

### Greek Symbols

|             |                                  |
|-------------|----------------------------------|
| $\alpha$    | thermal diffusivity, $m^2/s$     |
| $\beta$     | contact angle, $deg$             |
| $\lambda_c$ | cut-off wavelength, $\mu m$      |
| $\mu$       | dynamic viscosity, $kg/m\cdot s$ |
| $\nu$       | kinematic viscosity, $m^2/s$     |
| $\rho$      | density, $kg/m^3$                |
| $\sigma$    | surface tension, $N/m$           |

### Subscripts

|       |                     |
|-------|---------------------|
| $c$   | critical            |
| $cu$  | copper              |
| $exp$ | experimental        |
| $f$   | filtered profile    |
| $g$   | gas                 |
| $l$   | liquid              |
| $i$   | $i$ th value        |
| $o$   | reference condition |
| $pre$ | predicted           |
| $r$   | reduced property    |
| $ref$ | reference fluid     |
| $s$   | saturation          |
| $w$   | wall                |

### REFERENCES

- [1] Gorenflo, D., Chandra, U., Kottoff, S., and Luke, A., Influence of Thermophysical Properties on Pool Boiling of Refrigerants, *International Journal of Refrigeration*, vol. 27, pp. 492–502, 2004.
- [2] Jones, B. J., McHale, J. P., and Garimella, S. V., The Influence of Surface Roughness on Nucleate Pool Boiling Heat Transfer, *Journal of Heat Transfer*, vol. 131, pp. 1–14, 2009.

- [3] Kim, Y. H., Lee, K. J., and Han, D., Pool Boiling Enhancement With Surface Treatments, *Heat and Mass Transfer*, vol. 45, pp. 55–60, 2008.
- [4] McGillis, W. R., Carey, V. P., Fitch, J. S., and Hamburg, W. R., Pool Boiling Enhancement Techniques for Water at Low Pressure, *Seventh IEEE Semi-Therm Symposium*, pp. 64–72, 1991.
- [5] Yu, C. K., and Lu, D. C., Pool Boiling Heat Transfer on Horizontal Rectangular Fin Array in Saturated FC-72, *International Journal of Heat and Mass Transfer*, vol. 50, pp. 3624–3637, 2007.
- [6] Scurlock, R. G., Enhanced Boiling Heat Transfer Surfaces, *Cryogenics*, vol. 35, pp. 233–237, 1995.
- [7] Rainey, K. N., and You, S. M., Effects of Heater Size and Orientation in Pool Boiling Heat Transfer From Microporous Coated Surfaces, *International Journal of Heat and Mass Transfer*, vol. 44, pp. 2589–2599, 2001.
- [8] Stephan, K., and Abdelsalam, M., Heat Transfer Correlation for Natural Convection Boiling, *International Journal of Heat and Mass Transfer*, vol. 23, pp. 73–87, 1980.
- [9] Cooper, M. G., Saturation Nucleate Pool Boiling—A Simple Correlation, *ICHEME Symposium Series*, vol. 86, pp. 786–793, 1984.
- [10] Gorenflo, D., and Kenning, D. B. R., H2 Pool Boiling, in *VDI Heat Atlas*, Springer-Verlag, Berlin, 2009.
- [11] Jung, D., Kim, Y., Ko, Y., and Song, K., Nucleate Boiling Heat Transfer Coefficients of Pure Halogenated Refrigerants, *International Journal of Refrigeration*, vol. 26, pp. 240–248, 2003.
- [12] Shekrladze, I. G., Boiling Heat Transfer: Mechanisms, Models, Correlations and Lines of Further Research, *Open Mechanical Engineering Journal*, vol. 2, pp. 104–127, 2008.
- [13] Yagov, V. V., Nucleate Boiling Heat Transfer: Possibilities and Limitations of Theoretical Analysis, *Heat Mass Transfer*, vol. 45, pp. 881–892, 2009.
- [14] Rohsenow, W. M., A Method of Correlating Heat Transfer Data for Surface Boiling Liquids, *Transactions of ASME*, vol. 74, pp. 969–976, 1952.
- [15] Jabardo, J. M. S., Silva, E. F. D., Ribatski, G., and Barros, S. F. D., Evaluation of the Rohsenow Correlation Through Experimental Pool Boiling of Halocarbon Refrigerants on Cylindrical Surfaces, *Journal of the Brazilian Society of Mechanical Sciences and Engineering*, vol. 24, pp. 218–230, 2004.
- [16] Ahmad, S. W., *Combined Effect of Electric Field and Surface Modification on Pool Boiling of R-123*, Ph.D. thesis, Brunel University London, London, UK, 2012.
- [17] Ahmad, S. W., Karayiannis, T. G., Kenning, D. B. R., and Luke, A., Compound Effect of EHD and Surface Roughness in Pool Boiling and CHF With R-123, *Applied Thermal Engineering*, vol. 31, pp. 1994–2003, 2011.
- [18] Coleman, W. H., and Steele, G. W., *Experimentation and Uncertainty Analysis for Engineers*, John Wiley & Sons, New York, NY, 1989.
- [19] Pioro, I. L., Rohsenow, W., and Doerffer, S. S., Nucleate Pool Boiling Heat Transfer I: Review of Parametric Effects of Boiling Surface, *International Journal of Heat and Mass Transfer*, vol. 47, pp. 5033–5044, 2004.
- [20] Luke, A., Preparation, Measurement and Analysis of the Microstructure of Evaporator Surface, *International Journal of Thermal Sciences*, vol. 45, pp. 237–256, 2006.
- [21] Buxton, A. L., Ferhati, A., McGlen, R. J., Dance, B. G. I., Mullen, D., and Karayiannis, T. G., EB Surface Engineering for High Performance Heat Exchangers, *First International Electron Beam Welding Conference*, Chicago, IL, 2009.
- [22] Ahmad, S. W., Karayiannis, T. G., Lewis, J. S., McGlen, R. J., and Kenning, D. B. R., Pool Boiling on an Enhanced Surface, *12th UK National Heat Transfer Conference*, Leeds, UK, 2011.
- [23] Zaghdoudi, M. C., and Lallemand, M., Pool Boiling Heat Transfer Enhancement by Means of High DC Electric Field, *Arabian Journal for Science and Engineering*, vol. 30, pp. 189–212, 2005.
- [24] Hristov, Y., Zhao, D., Kenning, D. B. R., Sefiane, K., and Karayiannis, T. G., A study of Nucleate Boiling and Critical Heat Flux With EHD Enhancement, *Heat and Mass Transfer*, vol. 45, pp. 999–1017, 2009.
- [25] Luke, A., Preparation and Analysis of Different Roughness Structures for Evaporator Tubes, *Heat and Mass Transfer*, vol. 45, pp. 909–917, 2009.



**Syed W. Ahmad** obtained his Ph.D. from Brunel University London in 2012. He previously graduated in chemical engineering from the University of Engineering and Technology, Lahore, Pakistan, where he joined as a laboratory engineer. He is now an assistant professor in the Department of Polymer and Chemical Engineering at UET (Lahore). His research interests are in the field of single- and two-phase heat transfer.



**John S. Lewis** studied mechanical engineering at Lanchester College of Technology, Coventry, UK, and aircraft propulsion at the College of Aeronautics, Cranfield. He worked at the Engineering Sciences Data Unit on design data items for heat transfer and from 1972 to 2006 held academic positions at Middlesex University. He is now a visiting research fellow in the School of Engineering and Design at Brunel University. He received his Ph.D. from City University London in 1992 for research on combined convection

and has also worked on heat and mass transfer in spray systems and cooling towers. His current research is on single-phase and boiling heat transfer in microchannels. He is a member of the Institution of Mechanical Engineers and the Royal Aeronautical Society.



**Ryan J. McGlen** is a senior advanced technologies engineer at Thermacore Europe Ltd where he leads research into next-generation thermal technologies. He obtained a B.Eng. (hons.) degree in mechanical engineering at the University of Northumbria (UK) in 2002 and an industrial-based Ph.D. from the University of Newcastle (UK) in single- and two-phase heat transfer for cooling of microelectronics in 2007. He has more than 10 years of experience in thermal and mechanical design of commercial electronics cooling

systems and research and development projects. He is currently lead engineer on research and developments in next-generation heat pipe technology and advanced manufacturing techniques.



**Tassos G. Karayiannis** is a professor of thermal engineering in the School of Engineering and Design of Brunel University, where he is co-director of the Centre for Energy and Built Environment Research (CEBER). He obtained a B.Sc. in mechanical engineering from City University (UK) in 1981 and a Ph.D. from the University of Western Ontario (Canada) in 1986. He has carried out research in single-phase heat transfer, enhanced heat transfer, and thermal systems. He has been involved with research

in two-phase flow and heat transfer for about 20 years. He is a fellow of the Institution of Mechanical Engineers and the Institute of Energy.